Field moment expansion method for interacting bosonic systems

Andrew Eberhardt,[1,2,3,*] Michael Kopp,[4] Alvaro Zamora,[1,2,3] and Tom Abel[1,2,3]

[1]*Kavli Institute for Particle Astrophysics and Cosmology, Menlo Park, California 94025, USA*
[2]*Physics Department, Stanford University, Stanford, California 94305, USA*
[3]*SLAC National Accelerator Laboratory, Menlo Park, California 94025, USA*
[4]*Nordita, KTH Royal Institute of Technology and Stockholm University, Hannes Alfvéns väg 12, SE-106 91 Stockholm, Sweden*

(Received 24 August 2021; accepted 9 September 2021; published 5 October 2021)

We introduce a numerical method and PYTHON package, CHiMES, that simulates quantum systems initially well approximated by mean field theory using a second order extension of the classical field approach. We call this the field moment expansion method. In this way, we can accurately approximate the evolution of first and second field moments beyond where the mean field theory breaks down. This allows us to estimate the quantum break time of a classical approximation without any calculations external to the theory. We investigate the accuracy of the field moment expansion using a number of well studied quantum test problems. Interacting bosonic systems similar to scalar field dark matter are chosen as test problems. We find that successful application of this method depends on two conditions: the quantum system must initially be well described by the classical theory, and the growth of the higher order moments must be hierarchical.

DOI: 10.1103/PhysRevD.104.083007

I. INTRODUCTION

Interacting many body bosonic systems describe a wide array of interesting phenomena. This includes Bose-Einstein condensates (BEC) [1,2], electromagnetic radiation [3], and scalar field dark matter (SFDM) [4–6]. Their dynamical properties are often explored using a classical mean field theory (MFT) approximation, the Gross-Pitaevskii equations, or Schrödinger-Poisson equations in the case of SFDM [4,6–11].

Numerically, MFT is preferable to an exact quantum field description which, for a system with M interacting modes and total number of particles $n_{\rm tot}$, would involve simulating a Hilbert space of dimensional $\sim n_{\rm tot}^{M-2}$ [12]. For large M or $n_{\rm tot}$ an exact quantum treatment is infeasible. Rather than try and implement an exact quantum solver it is simpler to extend the classical theory using correction terms that capture quantum effects on the classical physics [13–19].

When occupation numbers are large and interactions weak, the MFT is known to accurately describe the dynamics of these systems [3,8,20–22]. However, any interacting system with a nonlinearity will exhibit quantum corrections on some timescale [18,23–28]. The MFT, tracking only the mean value of the field operator, cannot account for these quantum terms [13]. This means that effects such as phase diffusion, quantum squeezing, and fragmentation inherently require a beyond MFT approach [11,13,18,23]. The effect of these corrections on MFT is a current topic of interest [7,12,13,18,19,26,28–31]. This motivates the development of numerical methods which can capture beyond MFT physics [13–19]. We will refer to the time at which MFT can no longer accurately approximate the evolution of the underlying system as the "quantum break time."

The classical theory is generally achieved as a limit of the quantum field theory. When the expectation value of the field operator is large compared to the variance of the field operator, it is sensible to replace the field operators in the quantum field theory with their expectation values [32]. The expectation value of the quantum field is then called the classical field. Quantum coherent states, with parameters large compared to unity, satisfy this approximation criterion [32]. Tracking higher order moments and their effects on the evolution of observables has been studied with success for position and momentum operators [14,16]. Likewise, conceptually similar methods of expanding the field about its mean value have proven useful as corrections to MFT [17,19,33,34] as well as helping explore interesting physics [8,15,35,36].

We apply these techniques to extend the MFT approximation to include terms proportional to higher order central moments and then integrate coupled differential equations governing the evolution of the mean and these higher order moments. We will refer to this method as

*Corresponding author.
aeberhar@stanford.edu

the "field moment expansion" (FME). The main focus of this work will be to introduce a publicly available code repository which implements a solver which tracks both the mean field values and the second moments of the field. In this way we can simulate systems initially well described by MFT into regimes where quantum corrections become important.

There are two main benefits to this approach. First, prior to the quantum break time, FME produces a more accurate approximation of the quantum field expectation values than MFT. Second, FME provides an internal estimation of the break time and can therefore estimate its own regime of validity. This internal assessment means no calculations external to the theory are necessary to estimate the quantum break time. This is in contrast to approximations of this timescale calculated by methods external to MFT (see for example [29,30,37]). Additionally, when compared with other mean field extensions [13], the FME scales as $\mathcal{O}(M^2 \log M)$, depending only on the grid size as opposed to the particle occupation numbers n_p.

The method is applicable to any interacting scalar field system assuming that a number of criteria are met. First, the initial correction terms must be subleading order. The method predictions cannot be trusted past the time when the quantum corrections become large. However, we will show that the FME is able to approximate the evolution of the quantum system longer than MFT. Second, the correction terms must grow hierarchically. For a term, F of order m written as a function of moments of order less than and equal to m, given $F^m(\text{moments of order} \leq m)$, the evolution the terms must satisfy $F^1 > F^2 > F^3 \cdots$. Generally, these criteria will be met if the initial conditions are a coherent state with large mode occupation numbers.

In this work we test the field moment expansion using two test problems that have been well studied in the literature, for which exact quantum solutions are possible and that exhibit a breakdown of the MFT on some timescale [7,12,23,38]. For each we show that the FME provides a more accurate solution until the quantum break time. Most importantly, we demonstrate that the method can be used in this case to accurately predict the quantum break time.

The paper is organized as follows. In Sec. II, we discuss the background on interacting bosonic systems, the MFT, and FME approximations. Section III explains our numerical implementation. In Sec. IV, we demonstrate that FME is accurate for a number of quantum test problems. Conclusions regarding the overall utility of these methods and future directions are presented in Sec. V.

II. BACKGROUND

A. Quantum description

We start from the following Hamiltonian, used to describe nonrelativistic scalar fields [7,12,38]:

$$\hat{H} = \sum_j^M \omega_j \hat{a}_j^\dagger \hat{a}_j + \sum_{ijkl}^M \frac{\Lambda_{kl}^{ij}}{2} \hat{a}_k^\dagger \hat{a}_l^\dagger \hat{a}_i \hat{a}_j, \tag{1}$$

where the sums are performed over the M system modes. For appropriately chosen Λ, ω, and M this Hamiltonian describes a wide range of physical systems. The first sum describes the kinetic energy of the system and the second the self-interactions. $\hat{a}_i$ is the annihilation operator on mode i, which is defined by its commutation and action on number eigenstates. A number eigenstate is written as

$$|\{n\}\rangle = |n_1, n_2, \ldots, n_M\rangle, \tag{2}$$

where n_i describes the number of particles occupying the ith mode. Here we will take the modes to represent momentum eigenstates with momentum p_i. The number eigenstates form an orthonormal basis such that $\langle n_j' | n_i \rangle = \delta_{ij}\delta_{nn'}$. We can now describe the $\hat{a}$ operators as follows:

$$[\hat{a}_i, \hat{a}_j] = 0, \tag{3}$$

$$[\hat{a}_i, \hat{a}_j^\dagger] = \delta_{ij}, \tag{4}$$

$$\hat{a}_j^\dagger |n_j\rangle = (n_j + 1)^{1/2} |n_j + 1\rangle, \tag{5}$$

$$\hat{a}_j |n_j\rangle = n_j^{1/2} |n_j - 1\rangle, \tag{6}$$

$$\hat{N}_j |n_j\rangle \equiv \hat{a}_j^\dagger \hat{a}_j |n_j\rangle = n_j |n_j\rangle. \tag{7}$$

The annihilation operator can also be used to define the complex quantum field $\hat{\psi}(x)$, which is related to $\hat{a}$ by Fourier transform,

$$\hat{\psi}(x) = \sum_i \hat{a}_i u_i^\dagger(x), \tag{8}$$

where $u_i^\dagger(x)$ is the eigenstate of the momentum operator with eigenvalue p_i. The Heisenberg equation describes the dynamics of these operators. For an arbitrary operator $\hat{A}$ with a time independent Hamiltonian the equation of motion is written

$$\partial_t \hat{A} = \frac{i}{\hbar} [\hat{H}, \hat{A}]. \tag{9}$$

Hereafter we set $\hbar \equiv 1$. We can now solve for the evolution of our field operators,

$$\partial_t \hat{a}_p = i[\hat{H}, \hat{a}_p] = -i \left[\omega_p \hat{a}_p + \sum_{ijl} \Lambda_{pl}^{ij} \hat{a}_l^\dagger \hat{a}_i \hat{a}_j \right]. \tag{10}$$

In this work we will be taking the constants Λ_{pl}^{ij} to be of the following form:

$$\Lambda^{ij}_{pl} = \left(\frac{C}{2(p_p - p_i)^2} + \frac{C}{2(p_p - p_j)^2} + \Lambda_0\right)\delta^{ij}_{pl}, \quad (11)$$

where the constant C describes a long range r^{-1} potential and Λ_0 characterizes the strength of contact interactions. δ^{ij}_{pl} is the Kroneker delta. If $C = \frac{-4\pi G m^2}{L}$ and $\Lambda_0 = 0$, then taking a Fourier transform of Eq. (33) yields the familiar second quantized Schrödinger-Poisson equations, where G is the gravitational constant, L is the volume of the box for which the quantum field is periodic, and m is the mass of the field. Here we are working in one dimension (1D),

$$\partial_t \hat{\psi}(x) = -i\left[\frac{-\nabla^2}{2m} + m\hat{V}(x)\right]\hat{\psi}(x), \quad (12)$$

$$\nabla^2 \hat{V} = 4\pi G m \hat{\psi}^\dagger(x)\hat{\psi}(x). \quad (13)$$

Here we have started with a complex quantum field operator. However, it is possible to derive this set of equations as a nonrelativistic and weak gravity limit of the real scalar Klein Gordon field. This can be done following the derivation in [19,39]. These limits need to be kept in mind when determining where this set of equations and approximations of it are valid.

While the above analysis is true for an arbitrary quantum state, within the stated limits, it is useful to define an initial quantum state for which the mean field theory starts as an accurate approximation of the quantum field theory. The "most classical" state is the coherent state, for which MFT is initially exact, parametrized by the complex vector $\vec{z} \in \mathbb{C}^M$, which can be written as a sum of number eigenstates as

$$|\vec{z}\rangle = \bigotimes_{i=1}^{M} \exp\left[-\frac{|z_i|^2}{2}\right] \sum_{n_i=0}^{\infty} \frac{z_i^{n_i}}{\sqrt{n_i!}} |n_i\rangle. \quad (14)$$

When representing a coherent state numerically we truncate the above sum when the square norm of $\langle \vec{z}|\vec{z}\rangle \geq 0.995$.

A coherent state is thought to describe the initial state of the axion field if produced via the misalignment mechanism [40,41].

This state implies that a measurement of the particle number in the mode i would be Poisson distributed with expectation value $|z_i|^2$. This state is special because it has the property that the expectation value any normally ordered operator composed of $\hat{a}$ and $\hat{a}^\dagger$ with respect to this state is given by simply replacing the operators with the parameter z, i.e.,

$$\langle \vec{z}|f(\{\hat{a}^\dagger\})g(\{\hat{a}\})|\vec{z}\rangle = f(\vec{z}^\dagger)g(\vec{z}). \quad (15)$$

This will be important when deriving the mean field theory.

B. Mean field approximation

The mean field is simply the expectation value of the field operator; we define a mean field in position and momentum space, respectively, as

$$\psi(x) \equiv \langle \hat{\psi}(x)\rangle, \quad (16)$$

$$a_i \equiv \langle \hat{a}_i\rangle. \quad (17)$$

The higher order moments can then be calculated from the mean field operators. Occupation numbers, N^{cl}, are given as the amplitude of the field operators, e.g.,

$$N^{cl}_i = |a_i|^2. \quad (18)$$

The mean field theory is attained simply by taking an expectation value of the equations of motion and then approximating the operators by their expectation value. Let us say that the operator $\hat{A}$ evolves according to the following equation of motion:

$$\partial_t \hat{A} = f(\hat{A}). \quad (19)$$

And that $\hat{A}$ corresponds to some dynamic observable of the system. If the expectation value of $\hat{A}$ is large compared to its root variance, then we can make the following approximation:

$$\partial_t \langle \hat{A}\rangle = \langle f(\hat{A})\rangle \approx f(\langle \hat{A}\rangle). \quad (20)$$

This approximation is one way to transition to a mean field theory description. It is identical to the Ehrenfest theorem if we replaced the position and momentum operators with field operators.

This statement that the mean field theory is accurate at a time T implies the following conditions:

$$\mathrm{E}[\hat{A}(T)] \gg \sqrt{\mathrm{Var}[\hat{A}(T)]}. \quad (21)$$

Note this is a condition on both the evolution of the operator $\hat{A}$ and the quantum state that the expectation is taken with respect to.

For the mean field approximation to hold we need only that the approximation in Eq. (20) remain accurate on the timescale of the evolution. We will make the requirements more precise in the next section, but from here we can see qualitatively why a large occupation number tends to motivate the mean field theory approximation.

Let us assume that $\hat{A} = \{\hat{a}, \hat{a}^\dagger, \ldots\}$ is the set of operators generated by field operators $\hat{a}$ and $\hat{a}^\dagger$, as will be the case in the next sections. It is always possible to write the right-hand side of Eq. (19) in terms of normally ordered operators. This means that if we are in a coherent state by Eq. (15), the mean field approximation is an equality so

long as we remain in a coherent state. This is true regardless of the expected occupation number; however, if we are only in an approximately coherent state with $|z|^2 = n \gg 1$, then we can expect the variance in our field operators to be approximately governed by a Poisson distribution; i.e., $\mathrm{E}[\hat{N}] \sim \mathrm{Var}[\hat{N}] \sim |z|^2 = n$, and this means that the fractional deviation in the expectation value will go as $\sqrt{\mathrm{Var}[\hat{N}]}/\mathrm{E}[\hat{N}] \sim 1/\sqrt{N}$. This is easily made into an estimate of the fractional field variance by recalling that $\hat{N} = \hat{a}^\dagger \hat{a}$. So the fractional deviation in the field values is small for large occupation numbers $n \gg 1$.

Large occupation numbers are not enough on their own to ensure an accurate MFT description. The mean field theory will be accurate if the occupation numbers are large but also if the quantum state remains approximately coherent or, equivalently, if the distribution of the number operator has Poisson distributed expectation and variance proportional to some power of n. But the actual condition that needs to be satisfied is Eq. (21).

It is easy to imagine a state for which this assumption is not met. A number eigenstate, $|\{n\}\rangle$, for example has field expectation $\langle\{n\}|\hat{a}|\{n\}\rangle = 0$ even when $n \gg 1$. Therefore, it does not satisfy the condition in Eq. (21) and will not be well described by a single classical field even for large n. It was demonstrated in [12,27] that a number eigenstate did not approach a single classical field description even at a large occupation number. It was then shown in [7] that this state could be approximated by an ensemble of classical fields with ensembled expectation 0 and amplitude n.

It is important to note that alarge occupation number is only a proxy for the accuracy of the mean field theory. For example, a coherent state evolved by the free particle Hamiltonian will always be perfectly described by classical field theory even as $\mathrm{E}[\hat{N}] \ll 1$. Conversely, a number eigenstate will never be well described by a single classical field even as $\mathrm{E}[\hat{N}] \gg 1$. Going forward we will phrase our estimation of the accuracy of the classical field theory in terms of the condition described in Eq. (21) for the field operator $\hat{a}$.

It should also be noted that it is possible to reproduce the quantum evolution of the number operator without reproducing the evolution of the field itself. For example, a so-called field number state in the large N limit approaches the classical evolution of the mode occupations; however, it has a vanishing field expectation regardless of N. For states such as these, Eq. (21) should be expressed in terms of the number operator.

C. Quantum corrections

Systems initially well described by the mean field theory will eventually diverge from this description on some timescale if the Hamiltonian is nonharmonic. The specific causes of this are of interest in the literature [18,23–25,28] but for our purposes we can think of them generally as a delocalization in phase space. In this section we will show an example of how deviation from the classical field theory occurs and discuss a way to parametrize it.

Specifically that the variance in the field operators becomes of order the expectation value violating the condition in Eq. (21). We will clarify this point using the following example:

Consider the toy Hamiltonian on one mode,

$$\hat{H} = \frac{\hat{p}^2}{2m} + \lambda_L \hat{q}^2 + \lambda_{NL} \hat{q}^4, \tag{22}$$

where $p \equiv -i\hbar\nabla_q$. The first two terms define a harmonic oscillator and the last term some nonlinearity. The set of operators that we are interested in are the position and momentum operators $\hat{A} = \{\hat{q}, \hat{p}\}$. Note that this Hamiltonian can be recast in terms of the $\hat{a}$ operator using the relation

$$\hat{a} = \frac{1}{\sqrt{2}}(\hat{q} + i\hat{p}), \tag{23}$$

but this does not change the analysis.

The classical equations of motion can be found using Eqs. (9) and (22) as well as the commutation relation $[q, p] = i\hbar$ and then applying Ehrenfest's theorem. For the classical variables p, q related to the classical field by $a = \frac{1}{\sqrt{2}}(q + ip)$ (recall there is only a single mode), we obtain the following equations of motion:

$$\partial_t p = -2\lambda_L q - 4\lambda_{NL} q^3, \tag{24}$$

$$\partial_t q = p, \tag{25}$$

with $(q, p)|_{t=0} = (q_i, 0)$. We use a symplectic leapfrog integrator to solve the classical equations of motion.

Our initial wave function will be Gaussian, which is initially well localized in q,

$$\langle q|\phi\rangle = \sqrt{\frac{1}{\sqrt{2\pi}\sigma}} \exp\left(-\frac{(q - q_i)^2}{4\sigma^2}\right). \tag{26}$$

The quantum equations can be solved by integrating Schrödinger's equation

$$\partial_t |\phi\rangle = -i\hat{H}|\phi\rangle. \tag{27}$$

We use a symplectic spectral leapfrog integrator to perform the integration.

Let us also parametrize the inequality in Eq. (21) by defining the following quantity Q_q:

$$Q_q \equiv \frac{\langle \hat{q}^2 \rangle - \langle \hat{q} \rangle^2}{q_i^2}. \tag{28}$$

This can be used to parametrize the quantum theories' deviation from the classical theory because the nonlinearity is spatial. It should be noted that this is not the only parameter that can be constructed with this property.

In Fig. 1 we track a quantum phase space analog, the Husimi function [32], of the wave function, the classical mean field theory approximation of $\mathrm{E}[\hat{a}]$, the exact quantum value of $E[\hat{a}]$ for two different strength nonlinearities. In both cases the initial spread of the wave function is $\sigma = 0.025$, the initial location $q_i = 0.25$, $\hbar = 0.01$, $\lambda_L = 100$. This means that our parameter $Q_q = 0.01$. Note also that Eq. (23) implies that the occupation number here is $n = q_i^2 = 0.0625$. Clearly we are not in the high occupation regime. The top row and bottom rows have $\lambda_{\mathrm{NL}} = 0.073$ and $\lambda_{\mathrm{NL}} = 73$, representing the weakly nonlinear and strongly nonlinear, respectively.

For the nonlinear case we see in the second panel that squeezing and phase diffusion have caused the Husimi function to be poorly localized around the classical solution; however, at this time the Husimi function is still well approximated by a squeezed Gaussian. At this time the classical and quantum solutions begin to diverge. This is approximately the quantum break time, where the Q_q parameter is starting to approach $\mathcal{O}(1)$. In the rightmost panel of the nonlinear evolution we see that phase diffusion has removed most of the information about the phase of the field. The classical and quantum solutions now deviate by an $\mathcal{O}(1)$ fraction.

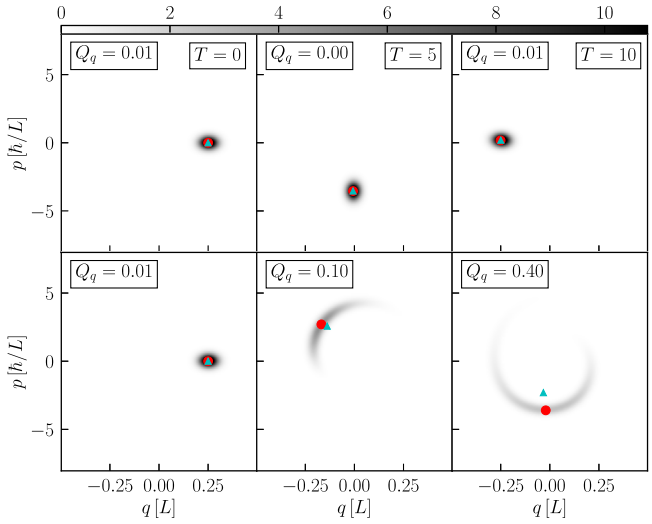

FIG. 1. Here we show how quantum corrections cause deviations from the mean field theory. Plotted are the Husimi functions for two different nonlinear models at three different times. The top row corresponds to the weakly nonlinear case with $\lambda_{NL} = 0.073$, and the bottom row to the strongly nonlinear case with $\lambda_{NL} = 73$. Each column corresponds to a different time T in the evolution. The red dot in each panel indicates the solution solved obtained using the classical mean field theory, a. The cyan triangle in each panel represents the actual mean of the $\hat{a}$ operator $\langle\hat{a}\rangle$. At all times the weakly nonlinear model closely adheres to the classical solution. The strongly nonlinear case has the classical field theory start as a good approximation but strongly diverge over the course of the evolution.

Throughout this work we will be interested in functions of the field operators and their Fourier transforms. We will define the quantum break time as we have done in this section, by first defining a quantity that parametrizes the deviation from the classical theory. The following definition will be used moving forward:

$$Q \equiv \sum_i^M \frac{\langle \delta\hat{a}_i^\dagger \delta\hat{a}_i \rangle}{n_{\mathrm{tot}}}, \tag{29}$$

where $n_{\mathrm{tot}} \equiv \sum_i^M n_i$ and $\delta\hat{a} \equiv \hat{a} - \langle\hat{a}\rangle$.

When Q is small, a single classical field can accurately capture both the first and second moments of the field operator and the classical approximation in Eq. (18) is valid. When this parameter ceases being small, such a description inaccurately captures both the field and occupation number expectations. Therefore, we will use Q to define a quantum break time, t_{br} condition as when $Q = 0.15$, i.e.,

$$Q(t_{\mathrm{br}}) \equiv 0.15. \tag{30}$$

Note that this is not intended to be the unique usable definition of the quantum break time. It is only intended to allow us to quantify when the assumption in Eq. (18) breaks down. The specific value 0.15 is arbitrary and the scaling of the break time with the occupation number should be relatively insensitive to the specific choice of $Q(t_{\mathrm{br}})$. We choose this specific value because it indicates that the correction terms are becoming the same order as the leading order classical terms and analysis of our test problems indicate that the field moment solver reliably reproduces quantum results when $Q < 0.15$.

D. Field moment expansion

For well-behaved probability distributions with well-defined moments, we can uniquely identify the distribution by its moments. This is true for functions of quantum mechanical operators. Consider a set of operators $\hat{A}$ and the function of this set $f(\hat{A})$. Let us assume we can write f as a sum of products of normally ordered generators of $\hat{A}$, and that there exists some integer R for which every term contains R or fewer elements of the generator of $\hat{A}$. Let us also assume that the ith moment of each element of $\hat{A}$ is well-defined for $i \leq R$. We can then write the expectation value of f as a sum of terms weighted by central moments as

$$\langle f(\hat{A})\rangle = f(\langle\hat{A}\rangle) + \sum_{j=2}^{R} \frac{1}{j!}\left[\prod_{k=1}^{j}\left(\sum_{\hat{a}\in\hat{A}} \hat{\delta}_{\hat{a}}\right)\right] f(\langle\hat{A}\rangle), \tag{31}$$

where $\langle \hat{A} \rangle \equiv \{\langle a_1 \rangle, \langle a_2 \rangle, \ldots\}$ is the set of the expectation values of the elements of the set $\hat{A}$ and the product of the $\hat{\delta}_{\hat{a}}$ operators is defined as

$$\hat{\delta}_{\hat{a}_1}\hat{\delta}_{\hat{a}_2}\ldots \equiv \langle \delta\hat{a}_1\delta\hat{a}_2\cdots\rangle \frac{\partial}{\partial\langle\hat{a}_1\rangle}\frac{\partial}{\partial\langle\hat{a}_2\rangle}\cdots, \tag{32}$$

where the operators $\delta\hat{a}$ are normally ordered.

Consider the Hamiltonian in Eq. (1). We can solve for the equation of motion for the $\hat{a}$ operator using Eq. (9) giving

$$\partial_t \hat{a}_p = i[\hat{H}, \hat{a}_p] = -i\left[\omega_p \hat{a}_p + \sum_{ijl} \Lambda^{ij}_{pl} \hat{a}^\dagger_l \hat{a}_i \hat{a}_j\right]. \tag{33}$$

We see that the highest order operator in the equation of motion is third order in $\hat{a}$ and $\hat{a}^\dagger$. Replacing the $\hat{a}$ and $\hat{a}^\dagger$ operators with their expectation values in this equation gives the classical field theory given by the following inequality:

$$\begin{aligned}\partial_t\langle\hat{a}_p\rangle &= i\langle[\hat{H}, \hat{a}_p]\rangle \\ &= -i\left[\omega_p\langle\hat{a}_p\rangle + \sum_{ijl}\Lambda^{ij}_{pl}\langle\hat{a}^\dagger_l\hat{a}_i\hat{a}_j\rangle\right] \qquad (34)\\ &\approx -i\left[\omega_p\langle\hat{a}_p\rangle + \sum_{ijl}\Lambda^{ij}_{pl}\langle\hat{a}^\dagger_l\rangle\langle\hat{a}_i\rangle\langle\hat{a}_j\rangle\right]. \qquad (35)\end{aligned}$$

We can rewrite Eq. (34) in the form of Eq. (31),

$$\begin{aligned}\partial_t\langle\hat{a}_p\rangle &= i\langle[\hat{H}, \hat{a}_p]\rangle \\ &= -i\left[\omega_p\langle\hat{a}_p\rangle + \sum_{ijl}\Lambda^{ij}_{pl}\langle\hat{a}^\dagger_l\hat{a}_i\hat{a}_j\rangle\right] \\ &= -i\Big[\omega_p\langle\hat{a}_p\rangle + \sum_{ijl}\Lambda^{ij}_{pl}(\langle\hat{a}^\dagger_l\rangle\langle\hat{a}_i\rangle\langle\hat{a}_j\rangle \qquad (36a)\\ &\quad + \langle\delta\hat{a}_i\delta\hat{a}_j\rangle\langle\hat{a}^\dagger_l\rangle + \langle\delta\hat{a}^\dagger_l\delta\hat{a}_i\rangle\langle\hat{a}_j\rangle + \langle\delta\hat{a}^\dagger_l\delta\hat{a}_j\rangle\langle\hat{a}_i\rangle \qquad (36b)\\ &\quad + \langle\delta\hat{a}^\dagger_l\delta\hat{a}_i\delta\hat{a}_j\rangle)\Big] \qquad (36c)\\ &\approx -i\Big[\omega_p\langle\hat{a}_p\rangle + \sum_{ijl}\Lambda^{ij}_{pl}(\langle\hat{a}^\dagger_l\rangle\langle\hat{a}_i\rangle\langle\hat{a}_j\rangle + \langle\delta\hat{a}_i\delta\hat{a}_j\rangle\langle\hat{a}^\dagger_l\rangle \\ &\quad + \langle\delta\hat{a}^\dagger_l\delta\hat{a}_i\rangle\langle\hat{a}_j\rangle + \langle\delta\hat{a}^\dagger_l\delta\hat{a}_j\rangle\langle\hat{a}_i\rangle)\Big]. \qquad (36d)\end{aligned}$$

We see in this form that the classical equations of motion are given by Eqs. (36a), and then (36b) and (36c) act as "quantum" corrections to the mean field theory. We can also see now the manner in which our classicality condition in Eq. (21) is technically imprecise. What is actually required is that the terms in (36b) and (36c) remain small compared to the terms in (36a). However, it is important to keep in mind that the accuracy of the mean field theory is not intrinsically a function of the occupation number but instead a property of how the moments of the field operators compare.

The condition in Eq. (21) comes about by assuming that the moments grow hierarchically; that is, that the first order terms in (36a) start out the largest and that the terms in (36b) grow faster than the terms in (36c) and so on. If we then also assume that the second order central moments in (36b) are all approximately the same order, and that the dynamics are approximately number conserving, we see that taking a ratio of the first and second order terms gives us the parameter Q and asserting that $Q \ll 1$ is equivalent then to Eq. (21).

In order to integrate Eq. (36) we couple the evolution of the field operator $\hat{a}$ to the evolution of the central moments. If we assume that the central moments grow hierarchically and we are interested in evolution only until the classical field theory breaks, we can truncate Eq. (36) at the second order terms; this has the benefit of better computational scaling. The equations of motion for the higher order moments can be found using Eq. (9) and then expanding to second order using Eq. (31). We will start with the $\mathrm{Cov}[\hat{a}_i, \hat{a}_j]$ operator which has the following equation of motion:

$$\begin{aligned}\partial_t\langle\delta\hat{a}_i\delta\hat{a}_j\rangle \approx -i\Big[&(\omega_i+\omega_j)\langle\delta\hat{a}_i\delta\hat{a}_j\rangle + \sum_{kp}\Lambda^{kp}_{ji}\langle\hat{a}_k\rangle\langle\hat{a}_p\rangle \\ &+ \sum_{kpl}\Lambda^{kp}_{ji}(\langle\delta\hat{a}_l\delta\hat{a}_j\rangle\langle\hat{a}^\dagger_k\rangle\langle\hat{a}_p\rangle \\ &+ \langle\delta\hat{a}_j\delta\hat{a}_p\rangle\langle\hat{a}^\dagger_k\rangle\langle\hat{a}_l\rangle + \langle\delta\hat{a}^\dagger_k\delta\hat{a}_j\rangle\langle\hat{a}_l\rangle\langle\hat{a}_p\rangle) \\ &+ (i\leftrightarrow j)\Big]. \qquad (37)\end{aligned}$$

This equation can be broken down into three types of terms. The first term and the second line of terms are the kinetic and potential terms, respectively. The terms are proportional to the covariance operator. The second term on the second line is proportional to both the potential energy and $[\hat{a}, \hat{a}^\dagger]$. This term guarantees that the covariance operator will grow even if initially zero so long as there is some nonlinearity in the Hamiltonian.

We can solve for the $\mathrm{Cov}[\hat{a}^\dagger_i, \hat{a}_j]$ operator in the same manner,

$$\partial_t\langle\delta\hat{a}_i^\dagger\delta\hat{a}_j\rangle \approx i\Big[(\omega_i-\omega_j)\langle\delta\hat{a}_i^\dagger a_j\rangle + \sum_{kpl}\Lambda_{ji}^{kp}(\langle\delta\hat{a}_j\delta\hat{a}_k\rangle\langle\hat{a}_p^\dagger\rangle\langle\hat{a}_l^\dagger\rangle + \langle\delta\hat{a}_p^\dagger\delta\hat{a}_j\rangle\langle\hat{a}_l^\dagger\rangle\langle\hat{a}_k\rangle + \langle\delta\hat{a}_l^\dagger\delta\hat{a}_l\rangle\langle\hat{a}_p^\dagger\rangle\langle\hat{a}_k\rangle) + (\text{c.c.}, i\leftrightarrow j)\Big], \tag{38}$$

which has the same structure as the previous equation without the term proportional to the commutation operator. c.c. indicates complex conjugate.

The term in Eq. (37) proportional to the commutation between $\hat{a}$ and $\hat{a}^\dagger$ gives us a qualitative sense of how a large occupation number implies classicality. If the quantum state is approximately coherent, then these second order central moments are near 0 by Eq. (15). On a timescale $\sim\mathcal{O}(\Lambda^{-1})$ the second order central moments will have grown by a factor of $[\hat{a},\hat{a}^\dagger]=1$. In the large occupation number limit $[\hat{a},\hat{a}^\dagger]=1\ll 1$, meaning our lowest order quantum corrections contribute vanishingly to the evolution of the mean field.

E. Penrose-Onsager criterion

When the Penrose-Onsager (PO) criterion [42] is satisfied, we can write

$$\langle\hat{a}_i^\dagger\hat{a}_j\rangle = \vec{z}_i^\dagger\vec{z}_j. \tag{39}$$

That is, that the expectation values of the second field moment matrix $M_{ij}\equiv\langle\hat{a}_i^\dagger\hat{a}_j\rangle$ can be written as an outer product of a single vector $\vec{z}$ with its complex conjugate.

When the PO criterion is satisfied, $\hat{M}_{ij}$ contains a single nonzero eigenvalue, called the principal eigenvalue, equal to the square norm of $\vec{z}$, i.e., $\lambda_p=\sum_i|z_i|^2$, where $\vec{z}/\sqrt{\sum_i|z_i|^2}$ is the corresponding principal eigenvector, $\vec{\xi}_p$. This vector is not *a priori* equal to the classical field, but when the classical field adequately describes the system, we expect the PO criterion to be satisfied.

Note that $\mathrm{Tr}[\hat{M}_{ij}]=n_{\mathrm{tot}}$ and, therefore, in number preserving systems the trace of $\hat{M}_{ij}$ is a conserved quantity. When the system is well described by the classical theory, we expect that the principal eigenvalue is very close to n_{tot}, and more specifically we expect [8]

$$\frac{\lambda_p}{n_{\mathrm{tot}}}-1\ll 1. \tag{40}$$

Because the FME tracks both second central moments $\langle\delta\hat{a}_i^\dagger\delta\hat{a}_j\rangle$ and $\langle\hat{a}_i\rangle$, we can use this method to approximate $\hat{M}_{ij}$ as

$$\hat{M}_{ij}^{\mathrm{FME}} = \langle\delta\hat{a}_i^\dagger\delta\hat{a}_j\rangle^{\mathrm{FME}} + (\langle\hat{a}_i\rangle^\dagger\langle\hat{a}_j\rangle)^{\mathrm{FME}}. \tag{41}$$

It is important to note that while both Q and Eq. (40) parametrize the deviation from the classical theory the two are technically distinct in the following way:

When $Q\ll 1$, it implies that the classical approximation in Eq. (18) is breaking down, i.e., $Q\sim 1,\to|\langle\hat{a}\rangle|^2\neq\langle\hat{a}^\dagger\hat{a}\rangle$. Note that this is not a useful parametrization for states which track the evolution of the mode occupations but not the field values themselves. On the other hand, $\lambda_p/n_{\mathrm{tot}}-1\ll 1$ implies that $\hat{M}_{ij}$ cannot be described by a single eigenvector. Neither explicitly implies that the classical field poorly approximates occupation numbers, but both can be used to give an approximate sense of how closely a system is adhering to the classical field theory.

III. NUMERICAL IMPLEMENTATION

A. Mean field theory

The evolution of the mean field, a^{cl}, is solved by integrating the classical field equations of motion given by

$$\partial_t a_p^{cl} = -i\Big[\omega_p a_p^{cl} + \sum_{ijl}\Lambda_{ji}^{kp}a_l^{cl\dagger}a_i^{cl}a_j^{cl}\Big]. \tag{42}$$

The initial conditions are chosen such that the field values correspond to a coherent state with parameter $\vec{z}=\vec{a}^{cl}$. Note that this implies the initial square amplitudes of the classical field give the mode occupation number expectations, i.e.,

$$|a_p^{cl}|^2|_{t=0} = E[\hat{N}_p]. \tag{43}$$

We use a fourth order Runga-Kutta update scheme to update the field [43,44]. The update function for the field at mode p is given as

$$F(a_p) = a_p(1-i\omega_p\Delta t) - if(a)_p\Delta t, \tag{44}$$

and the update scheme is then

(1) $k_1=F(a_p^{cl}(t))$
(2) $k_2=F(a_p^{cl}(t)+k_1/2)$
(3) $k_3=F(a_p^{cl}(t)+k_2/2)$
(4) $k_4=F(a_p^{cl}(t)+k_3)$
(5) $a_p^{cl}(t+\Delta t)=\frac{1}{6}(k_1+2k_2+2k_3+k_4)$,

which takes the field at a time t, $a^{cl}(t)$, to a time $t+\Delta t$, $a^{cl}(t+\Delta t)$. The function $f(a)$ defines the potential term and is given as follows:

$$f(a)_p = \mathcal{F}[V(x)\psi(x)]_p,$$
$$V(x) = \mathcal{F}^{-1}\Big[\mathcal{F}[\psi^\dagger(y)\psi(y)]_i\Big(\frac{C}{k_i^2}+\Lambda_0\Big)\Big](x), \tag{45}$$

where $\mathcal{F}$ and $\mathcal{F}^{-1}$ define the Fourier transform and inverse Fourier transform, respectively. $\psi(x) = \sum_i a_i^{cl} u_i^\dagger(x)$, as in Eq. (8); i.e., ψ is the inverse Fourier transform of a^{cl}. In these simulations we use nonperiodic boundary conditions. This is achieved by padding the ends of the arguments of the Fourier transform with $M/2$ zeros, meaning our discrete Fourier transforms are defined as follows:

$$\mathcal{F}[\psi(x)]_p = \sum_{x=-M/2}^{M+M/2} \tilde{\psi}(x) u_p(x), \tag{46a}$$

$$\mathcal{F}^{-1}[a_p](x) = \sum_{p=-M/2}^{M+M/2} \tilde{a}_p u_p^\dagger(x), \tag{46b}$$

and the padded fields are given by

$$\tilde{\psi}(x) = \begin{cases} \psi(x) & 0 \le x \le M \\ 0 & \text{else} \end{cases}, \tag{47a}$$

$$\tilde{a}_p = \begin{cases} a_p & 0 \le p \le M \\ 0 & \text{else} \end{cases}. \tag{47b}$$

The unpadded fields can be recovered by looking only at the modes $\in [0, M]$.

B. Field moment expansion

The evolution of the field moments is solved by integrating the coupled equations (36d), (37), and (38). The initial conditions are chosen such that the initial values of the moments correspond to those of a coherent state with parameter $\vec{z}$. Meaning

$$\langle \hat{a}_p \rangle^{\text{FME}}|_{t=0} = z_p, \tag{48}$$

$$\langle \delta\hat{a}_i \delta\hat{a}_j \rangle^{\text{FME}}|_{t=0} = 0, \tag{49}$$

$$\langle \delta\hat{a}_i^\dagger \delta\hat{a}_j \rangle^{\text{FME}}|_{t=0} = 0. \tag{50}$$

This solver uses the following updated functions

$$F_a^{\text{FME}}(a_p, \delta A_{ij}, \delta B_{ij}) = a_p(1 - i\omega_p \Delta t) - i\Delta t(f(a^1)_p + g_1(a, \delta A_{ij})_p + g_2(a, \delta B_{ij})_p), \tag{51}$$

$$F_{aa}^{\text{FME}}(a_p, \delta A_{ij}, \delta B_{ij}) = \delta A_{ij}(1 - i(\omega_i + \omega_j)\Delta t) - i\Delta t(h(a)_{ij} + g_3(a, \delta A_{ij})_{ij} + g_4(a, \delta B_{ij})_{ij}), \tag{52}$$

$$F_{ba}^{\text{FME}}(a_p, \delta A_{ij}, \delta B_{ij}) = \delta B_{ij}(1 + i(\omega_i - \omega_j)\Delta t) - i\Delta t(g_5(a, \delta A_{ij})_{ij} + g_6(a, \delta B_{ij})_{ij}). \tag{53}$$

We use the following Runga-Kutta integration scheme to update the field moments:

(1) $k_1^a = F_a^{\text{FME}}(\langle \hat{a}_p \rangle^{\text{FME}}(t), \langle \delta\hat{a}_i \delta\hat{a}_j \rangle^{\text{FME}}(t), \langle \delta\hat{a}_i^\dagger \delta\hat{a}_j \rangle^{\text{FME}}(t))$
(2) $k_1^{aa} = F_{aa}^{\text{FME}}(\langle \hat{a}_p \rangle^{\text{FME}}(t), \langle \delta\hat{a}_i \delta\hat{a}_j \rangle^{\text{FME}}(t), \langle \delta\hat{a}_i^\dagger \delta\hat{a}_j \rangle^{\text{FME}}(t))$
(3) $k_1^{ba} = F_{ba}^{\text{FME}}(\langle \hat{a}_p \rangle^{\text{FME}}(t), \langle \delta\hat{a}_i \delta\hat{a}_j \rangle^{\text{FME}}(t), \langle \delta\hat{a}_i^\dagger \delta\hat{a}_j \rangle^{\text{FME}}(t))$
(4) $k_2^a = F_a^{\text{FME}}(\langle \hat{a}_p \rangle^{\text{FME}}(t) + k_1^a/2, \langle \delta\hat{a}_i \delta\hat{a}_j \rangle^{\text{FME}}(t) + k_1^{aa}/2, \langle \delta\hat{a}_i^\dagger \delta\hat{a}_j \rangle^{\text{FME}}(t) + k_1^{ba}/2)$
(5) $k_2^{aa} = F_{aa}^{\text{FME}}(\langle \hat{a}_p \rangle^{\text{FME}}(t) + k_1^a/2, \langle \delta\hat{a}_i \delta\hat{a}_j \rangle^{\text{FME}}(t) + k_1^{aa}/2, \langle \delta\hat{a}_i^\dagger \delta\hat{a}_j \rangle^{\text{FME}}(t) + k_1^{ba}/2)$
(6) $k_2^{ba} = F_{ba}^{\text{FME}}(\langle \hat{a}_p \rangle^{\text{FME}}(t) + k_1^a/2, \langle \delta\hat{a}_i \delta\hat{a}_j \rangle^{\text{FME}}(t) + k_1^{aa}/2, \langle \delta\hat{a}_i^\dagger \delta\hat{a}_j \rangle^{\text{FME}}(t) + k_1^{ba}/2)$
(7) $k_3^a = F_a^{\text{FME}}(\langle \hat{a}_p \rangle^{\text{FME}}(t) + k_2^a/2, \langle \delta\hat{a}_i \delta\hat{a}_j \rangle^{\text{FME}}(t) + k_2^{aa}/2, \langle \delta\hat{a}_i^\dagger \delta\hat{a}_j \rangle^{\text{FME}}(t) + k_2^{ba}/2)$
(8) $k_3^{aa} = F_{aa}^{\text{FME}}(\langle \hat{a}_p \rangle^{\text{FME}}(t) + k_2^a/2, \langle \delta\hat{a}_i \delta\hat{a}_j \rangle^{\text{FME}}(t) + k_2^{aa}/2, \langle \delta\hat{a}_i^\dagger \delta\hat{a}_j \rangle^{\text{FME}}(t) + k_2^{ba}/2)$
(9) $k_3^{ba} = F_{ba}^{\text{FME}}(\langle \hat{a}_p \rangle^{\text{FME}}(t) + k_2^a/2, \langle \delta\hat{a}_i \delta\hat{a}_j \rangle^{\text{FME}}(t) + k_2^{aa}/2, \langle \delta\hat{a}_i^\dagger \delta\hat{a}_j \rangle^{\text{FME}}(t) + k_2^{ba}/2)$
(10) $k_4^a = F_a^{\text{FME}}(\langle \hat{a}_p \rangle^{\text{FME}}(t) + k_3^a, \langle \delta\hat{a}_i \delta\hat{a}_j \rangle^{\text{FME}}(t) + k_3^{aa}, \langle \delta\hat{a}_i^\dagger \delta\hat{a}_j \rangle^{\text{FME}}(t) + k_3^{ba})$
(11) $k_4^{aa} = F_{aa}^{\text{FME}}(\langle \hat{a}_p \rangle^{\text{FME}}(t) + k_3^a, \langle \delta\hat{a}_i \delta\hat{a}_j \rangle^{\text{FME}}(t) + k_3^{aa}, \langle \delta\hat{a}_i^\dagger \delta\hat{a}_j \rangle^{\text{FME}}(t) + k_3^{ba})$
(12) $k_4^{ba} = F_{ba}^{\text{FME}}(\langle \hat{a}_p \rangle^{\text{FME}}(t) + k_3^a, \langle \delta\hat{a}_i \delta\hat{a}_j \rangle^{\text{FME}}(t) + k_3^{aa}, \langle \delta\hat{a}_i^\dagger \delta\hat{a}_j \rangle^{\text{FME}}(t) + k_3^{ba})$
(13) $\langle \hat{a}_p \rangle^{\text{FME}}(t + \Delta t) = \frac{1}{6}(k_1^a + 2k_2^a + 2k_3^a + k_4^a)$
(14) $\langle \delta\hat{a}_i \delta\hat{a}_j \rangle^{\text{FME}}(t + \Delta t) = \frac{1}{6}(k_1^{aa} + 2k_2^{aa} + 2k_3^{aa} + k_4^{aa})$
(15) $\langle \delta\hat{a}_i^\dagger \delta\hat{a}_j \rangle^{\text{FME}}(t + \Delta t) = \frac{1}{6}(k_1^{ba} + 2k_2^{ba} + 2k_3^{ba} + k_4^{ba})$,

which takes the field moments at time t, $\langle \hat{a} \rangle^{\text{FME}}(t)$, $\langle \delta\hat{a}_i \delta\hat{a}_j \rangle^{\text{FME}}(t)$, $\langle \delta\hat{a}_i^\dagger \delta\hat{a}_j \rangle^{\text{FME}}(t)$, to a time $t + \Delta t$, $\langle \hat{a} \rangle^{\text{FME}}(t + \Delta t)$, $\langle \delta\hat{a}_i \delta\hat{a}_j \rangle^{\text{FME}}(t + \Delta t)$, $\langle \delta\hat{a}_i^\dagger \delta\hat{a}_j \rangle^{\text{FME}}(t + \Delta t)$, where the functions are given by

$$g_1(a,\langle\delta a_i\delta a_j\rangle)_p = \mathcal{F}\left[\mathcal{F}^{-1}\left[\mathcal{F}_y[\langle\delta\psi(x)\delta\psi(y)\rangle\psi^\dagger(y)]_i\left(\frac{C}{k_i^2}+\Lambda_0\right)\right](x,x)\right]_p, \tag{54}$$

$$\begin{aligned} g_2(a,\langle\delta a_i^\dagger\delta a_j\rangle)_p = {}& \mathcal{F}\left[\mathcal{F}^{-1}\left[\mathcal{F}_x[\langle\delta\psi^\dagger(x)\delta\psi(y)\rangle\psi(x)]_i\left(\frac{C}{k_i^2}+\Lambda_0\right)\right](x,x)\right]_p \\ & + \mathcal{F}\left[\mathcal{F}^{-1}\left[\mathcal{F}[\langle\delta\psi^\dagger(x)\delta\psi(x)\rangle]_i\left(\frac{C}{k_i^2}+\Lambda_0\right)\right](x)\psi(x)\right]_p, \end{aligned} \tag{55}$$

$$h(a)_{ij} = \mathcal{F}_{xy}[K(x,y)\psi(x)\psi(y)]_{ij}, \tag{56}$$

$$\begin{aligned} g_3(a,\langle\delta a_i\delta a_j\rangle)_{ij} = {}& \mathcal{F}_{xy}\left[\mathcal{F}^{-1}\left[\mathcal{F}_y[\langle\delta\psi(x)\delta\psi(y)\rangle\psi^\dagger(x)]_i\left(\frac{C}{k_i^2}+\Lambda_0\right)\right](x,y)\psi(x)\right]_{ij} \\ & + \mathcal{F}_{xy}\left[\mathcal{F}^{-1}\left[\mathcal{F}[|\psi(x)|^2]_i\left(\frac{C}{k_i^2}+\Lambda_0\right)\right](x)\langle\delta\psi(x)\delta\psi(y)\rangle\right]_{ij} + (i\leftrightarrow j), \end{aligned} \tag{57}$$

$$g_4(a,\langle\delta a_i^\dagger\delta a_j\rangle)_{ij} = \mathcal{F}_{xy}\left[\mathcal{F}^{-1}\left[\mathcal{F}_x[\langle\delta\psi^\dagger(x)\delta\psi(y)\rangle\psi(x)]_i\left(\frac{C}{k_i^2}+\Lambda_0\right)\right](x,y)\psi(x)\right]_{ij} + (i\leftrightarrow j), \tag{58}$$

$$g_5(a,\langle\delta a_i\delta a_j\rangle)_{ij} = \mathcal{F}_{xy}\left[\mathcal{F}^{-1}\left[\mathcal{F}_x[\langle\delta\psi(x)\delta\psi(y)\rangle\psi^\dagger(x)]_i\left(\frac{C}{k_i^2}+\Lambda_0\right)\right](x,y)\psi^\dagger(x)\right]_{ij} - (\text{c.c.}, i\leftrightarrow j), \tag{59}$$

$$\begin{aligned} g_6(a,\langle\delta a_i^\dagger\delta a_j\rangle)_{ij} = {}& \mathcal{F}_{xy}\left[\mathcal{F}^{-1}\left[\mathcal{F}_x[\langle\delta\psi^\dagger(x)\delta\psi(y)\rangle\psi(x)]_i\left(\frac{C}{k_i^2}+\Lambda_0\right)\right](x,y)\psi^\dagger(x)\right]_{ij} \\ & + \mathcal{F}_{xy}\left[\mathcal{F}^{-1}\left[\mathcal{F}[|\psi(x)|^2]_i\left(\frac{C}{k_i^2}+\Lambda_0\right)\right](x)\langle\delta\psi^\dagger(x)\delta\psi(y)\rangle\right]_{ij} - (\text{c.c.}, i\leftrightarrow j). \end{aligned} \tag{60}$$

We again define our discrete Fourier transforms as in Eq. (46) in order to enforce nonperiodic boundary conditions. The position space fields are related to the momentum space arguments by

$$\psi(x) = \sum_i a_i u_i^\dagger(x), \tag{61}$$

$$\langle\delta\psi^\dagger(x)\psi(y)\rangle = \sum_{ij}\langle\delta\hat{a}_i^\dagger\delta\hat{a}_j\rangle u_i(x)u_j^\dagger(y), \tag{62}$$

$$\langle\delta\psi(x)\psi(y)\rangle = \sum_{ij}\langle\delta\hat{a}_i\delta\hat{a}_j\rangle u_i^\dagger(x)u_j^\dagger(y). \tag{63}$$

C. Quantum field theory

The evolution of the quantum system is solved by integrating Schrödinger's equation

$$\partial_t|\vec{z}\rangle = -i\hat{H}|\vec{z}\rangle. \tag{64}$$

We integrate this equation using the QIBS repository available at [45].

IV. TEST PROBLEMS

The purpose of this section is to compare the FME and MFT approximations of quantum systems using solutions which can be evaluated exactly, either analytically or numerically. In general, we will look to demonstrate that the field moment expansion is successful based on the following criteria:

(1) Provides a more accurate approximation of the expectation value of the field operator $\langle\hat{a}\rangle$ at least until the quantum break time as defined in Eq. (30).
(2) An accurate approximation of when the quantum break time occurs.

Note that the expectation values of the occupation numbers can be found using Q, n_{tot}, and $\langle\hat{a}\rangle$. Therefore, achieving the two goals listed above also implies that the field moment expansion can accurately approximate the expectation values of the occupation numbers.

A. Kerr nonlinearity

In this section we examine the Kerr nonlinearity which can be described by the following Hamiltonian:

$$\begin{aligned}\hat{H} &= \omega\hat{a}^\dagger\hat{a} + \frac{\Lambda_0}{2}(\hat{a}^\dagger\hat{a})^2 \\ &= \left(\omega + \frac{\Lambda_0}{2}\right)\hat{a}^\dagger\hat{a} + \frac{\Lambda_0}{2}\hat{a}^\dagger\hat{a}^\dagger\hat{a}\,\hat{a} \\ &= \omega_0\hat{a}^\dagger\hat{a} + \frac{\Lambda_0}{2}\hat{a}^\dagger\hat{a}^\dagger\hat{a}\,\hat{a}\,. \end{aligned} \tag{65}$$

This is a special case of our Hamiltonian in Eq. (1) with $C = 0$, $M = 1$.

This problem is interesting because it admits an exact solution, and so the timescales on which it diverges from the classical solution can be found analytically [23,36]. Our initial condition will be a coherent state; see Eq. (14). The exact wave function can be given as a function of time as follows:

$$|\phi(t)\rangle = \exp\left[-\frac{|z|^2}{2}\right]\sum_n e^{-it(\Lambda_0 n^2/2+\omega n)}\frac{z^n}{\sqrt{n!}}|n\rangle. \tag{66}$$

Given this, it is straightforward to calculate the exact evolution of the normally ordered central moments and the field expectation. The quantum evolution of the expectation of the field is characterized by a decaying amplitude which is not captured in the classical theory, as shown in the top left panel of Fig. 2. Here we set $z = 5$, $\Lambda = 1 \times 10^{-3}$, and $\omega = 1$.

The far left column of Fig. 3 shows the result of applying the field moment expansion to this system. We can see that Q effectively parametrizes the time when the fractional error in the classical theory is no longer small. Until this point the field moment expansion provides a solution with a much lower fractional deviation. Likewise, until the break time the field moment expansion estimate of Q remains accurate. Therefore, the field moment expansion both provides a more accurate solution until the break time and successfully provides an accurate estimation of this time.

The evolution central moments are shown in Fig. 4. As expected for an initially coherent state the central moments all start out at 0 and then grow on a timescale set by the nonlinearity. We see also that the moments grow hierarchically, with the second central moments, normalized by $|z|^3$, becoming $\sim\mathcal{O}(1)$ faster than the third central moment. We see both the initial accuracy of the mean field theory and the hierarchically growth conditions that are met for this system.

The field moment expansion remains more accurate, past the break time; however, we can see in Fig. 4 that past this time the third moment begins to become relevant. Since we have truncated our expansion at second order past this time, this is where we expect our solver to fail. Therefore, even assuming hierarchical growth, the field moment expansion is not reliable past the time when the highest moment in its truncation becomes large.

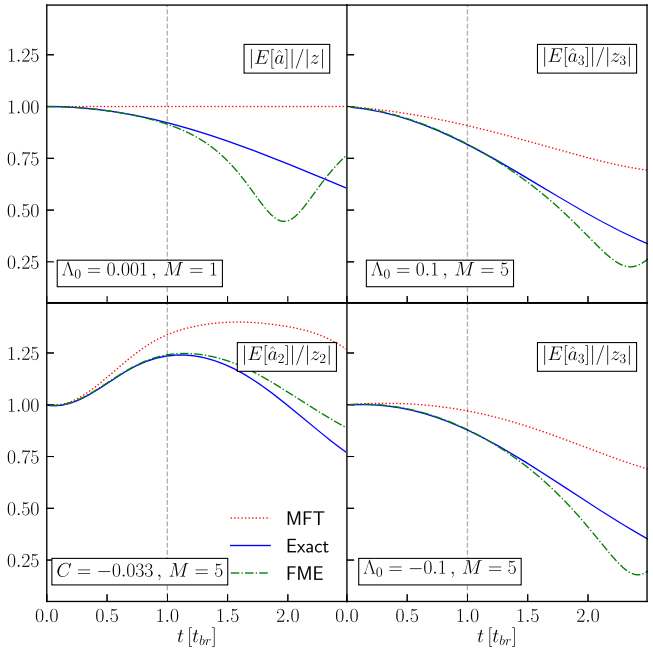

FIG. 2. Here we show the evolution of the mean field for a given more for each method in each of our test problems. The Kerr nonlinearity is shown in the top left. The repulsive and attractive contact interactions are in the top and bottom right, respectively. Attractive long range interactions are shown in the bottom left. Nonzero coupling constants and mode numbers are given in each panel. On the vertical axis we plot the absolute value of the expectation of one of the mode field operators as a fraction of the initial value. On the horizontal axis we plot the time as a fraction of the quantum break time. Therefore, $t = 1$ corresponds to the quantum break time in all plotted systems, shown by the dashed light gray line. In all cases, the classical field solution, shown in the dotted red line, has diverged from the exact quantum solution, shown in the solid blue line. However, the field moment expansion solution, shown in the dashed green line, remains an accurate approximation of the exact quantum solution at least until the break time.

B. Contact interactions

Unlike the previous test problem, scalar field dark matter systems involve a large number of modes. Therefore, it is prudent to test the accuracy of the field moment expansion on a system with multiple modes. We select the system given by the Hamiltonian in Eq. (1) with $M = 5$. This Hamiltonian has been used as a test problem in [7,12,38] and so will serve as a good benchmark to test the field moment expansion. It also contains a self-interaction term which is present in many models of scalar field dark matter.

This system models a contact interaction and linear dispersion, which implies the following:

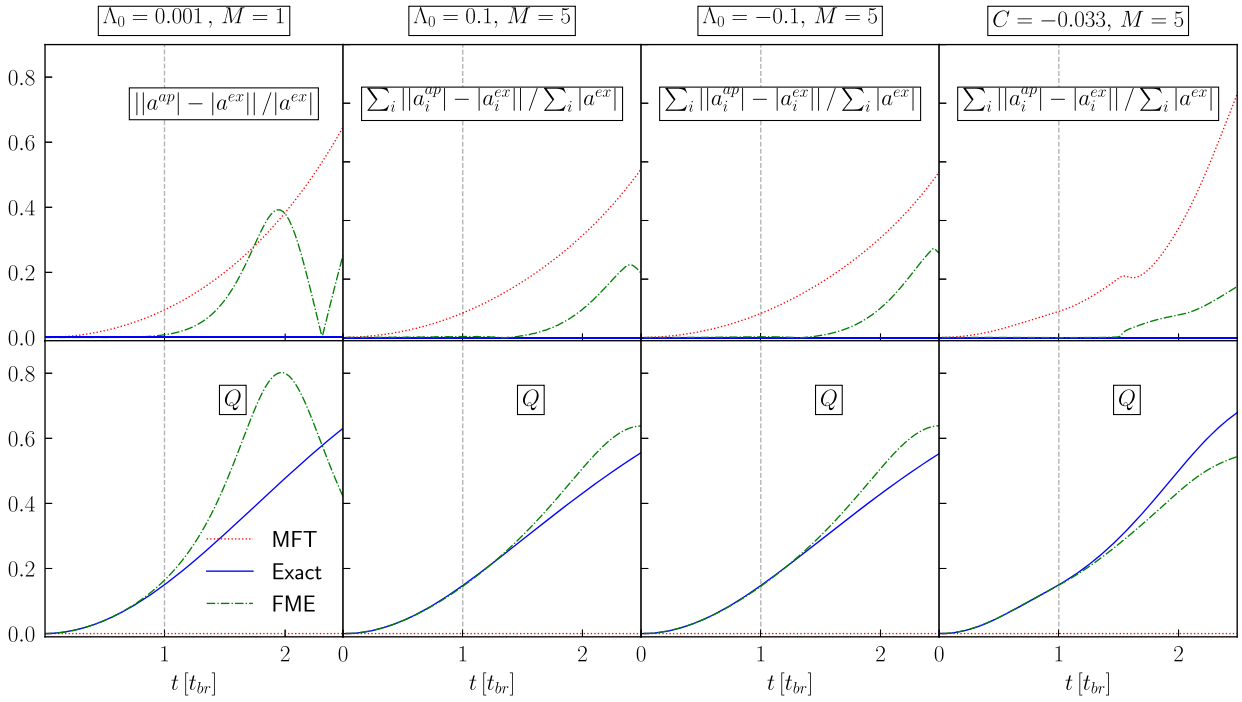

FIG. 3. Here we show the fractional error and approximation of Q for each method in each of our test problems. In the top row we show the error in each method's approximation of the magnitude of the mean field as a fraction of the exact value of the mean field. In the bottom row we show each method's approximation of Q. The Kerr nonlinearity is shown on the far left column. The repulsive and attractive contact interactions are in the middle left and right columns, respectively. Attractive long range interactions are shown in the far right column. Nonzero coupling constants and mode numbers are given above each column. On the horizontal axis we plot the time as a fraction of the quantum break time. Therefore, $t = 1$ corresponds to the quantum break time in all plotted systems, shown in the dashed light gray line. In all cases, the classical field, shown in the dotted red line, has a relatively large fractional error by the break time. However, the field moment expansion solution, shown in the dashed green line, remains an accurate approximation of the exact quantum solution, shown in the blue line, until at least the break time. Likewise, the field moment expansion accurately approximates Q until the break time.

$$\Lambda^{ij}_{pl} = \Lambda_0 \delta^{ij}_{pl}, \tag{67}$$

$$\omega_j = j\omega_0, \tag{68}$$

where $\Lambda_0 < 0$ defines an attractive interaction and $\Lambda_0 > 0$ a repulsive one. We evolve a coherent state defined by parameter $\vec{z} \in \mathbb{C}^5$. In order to test how the solution behaves with a scaled occupation number we will simulate a benchmark coherent state $|\vec{z}; r\rangle$ where $\vec{z} = (0, \sqrt{2r}e^{i\theta_1}, \sqrt{2r}e^{i\theta_2}, \sqrt{1r}e^{i\theta_3}, 0)$ and the phases are drawn from a uniform random distribution, $\theta_i \sim U[0, 2\pi)$ with a fixed random seed.

For this system, in general, the occupations of the modes will thermalize and the expectation of the field itself will decay. This is shown in the right two columns of Fig. 5. Here we set $\Lambda_0 = \pm 0.1$, $\omega_0 = 1$, $M = 5$, and $r = 3$.

We now test the field moment expansion to assess its accuracy and ability to approximate the quantum break time. As in the previous problem we can see that the field moment expansion solution remains close to the quantum solution past where the deviation between the classical field theory and quantum field theory becomes large. This is shown for mode 3 in the middle two columns of Fig. 2. The field moment expansion also successfully predicts the quantum break time. This is shown for $r = 3$ in the middle two columns of Fig. 3. We can see that the field moment expansion approximation of the field as well as the Q parameter remains accurate until past the break time. We use the field moment expansion to estimate the break time for a number of different values of r. This is shown for the repulsive and attractive potentials in the top and middle panels, respectively, of Fig. 6. There we also show an approximation of the break time using the PO condition. The results of the two break time definitions approximately agree. We see that the field moment expansion closely approximates the break time in all cases.

C. Long range interactions

SFDM can include self-interactions such as those in the previous section. However, given that we expect dark matter to be nearly collisionless, long range interactions such as those found in gravity are going to govern much of the evolution. Therefore, we now turn toward modeling a system with a $1/r$ potential.

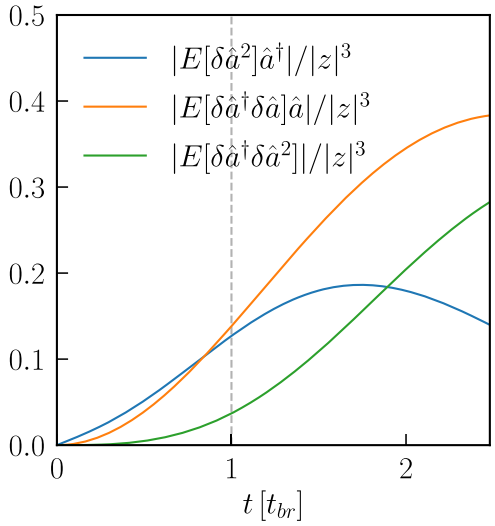

FIG. 4. Here we show the evolution of the central field moments, normalized by $|z|^3$, over time. We see all three moments become $\sim\mathcal{O}(1)$ on a timescale set by the nonlinearity. The second moments become relatively large by the quantum break time, shown in the dashed light gray line. The moments growth is hierarchical; i.e., the second moments become large before the third moment. Here we set $z = 5$, $\Lambda = 1 \times 10^{-3}$, and $\omega = 1$.

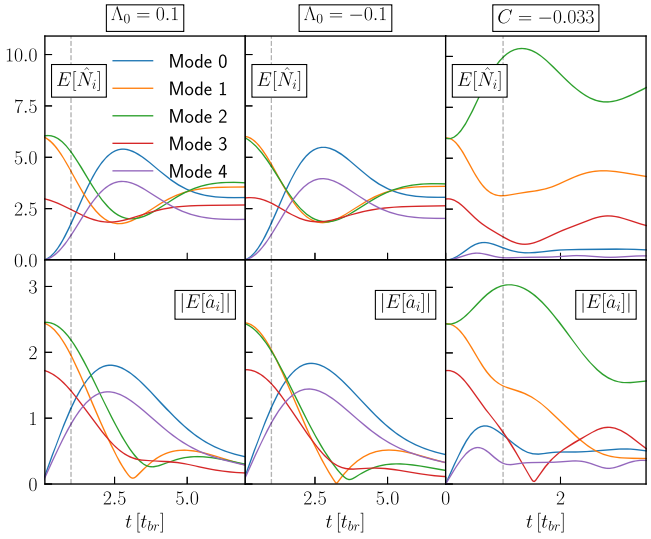

FIG. 5. Here we plot the evolution of the expectation of the number and field operators. In the top row we show the expectation value of the occupation of each mode. In the bottom row we show the amplitude of the expectation of the field operator. In general this amplitude decays over time due to quantum effects such as phase diffusion. The middle and left columns show the results of simulating contact interactions. The left column shows the repulsive case with $\Lambda_0 > 0$ and the middle column the attractive case with $\Lambda_0 < 0$. The rightmost column shows evolution of the long range attractive interactions. For reference, the quantum break time for each system is shown in the dashed light gray line. Nonzero nonlinear parameters are given above each column. In all cases $\omega_0 = 1$, $M = 5$, and $r = 3$.

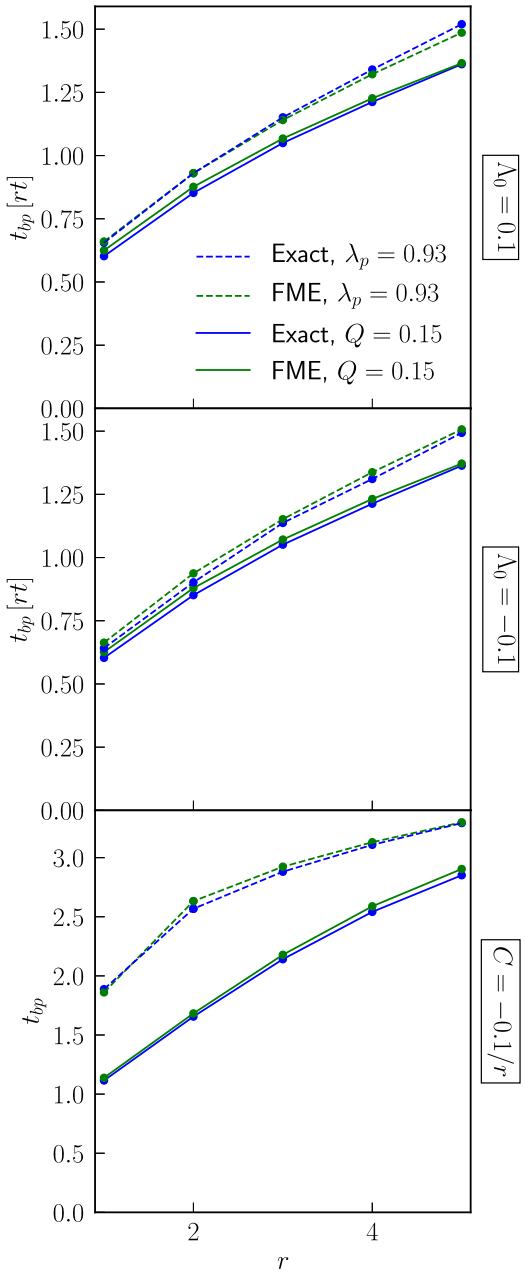

FIG. 6. Here we show FME, in the green line, estimate of the break time compared to the exact quantum result, in the blue line, for a number of r values. We show both the results of an analysis using Q and the PO condition, dashed and solid lines, respectively. We see that FME provides a close estimate of the break time. Here we set $\omega_0 = 1$, $M = 5$.

We still start with the Hamiltonian described in Eq. (1). As in contact interaction test problems we will use $M = 5$. Long range interactions and a quadratic dispersion relation can be modeled using the following constants:

$$\Lambda^{ij}_{pl} = \left(\frac{C}{2(p_p - p_i)^2} + \frac{C}{2(p_p - p_j)^2}\right)\delta^{ij}_{pl}, \qquad (69)$$

$$\omega_j = \frac{j^2}{2}\omega_0, \tag{70}$$

where again $C < 0$ gives an attractive potential and $C > 0$ a repulsive one. Here we evolve the same benchmark coherent state, $|\vec{z}; r\rangle$, as the last section, where $\vec{z} = (0, 2re^{i\theta_1}, 2re^{i\theta_2}, 1re^{i\theta_3}, 0)$ and the phases are drawn from a uniform random distribution, $\theta_i \sim U[0, 2\pi)$ with fixed random seed.

The density of dark matter is well measured [46]. And therefore the quantity $n_{\rm tot}C$ should be fixed as we vary the occupation number. This means that larger occupation results in a lower value of C. As we scale our reference state, then we will also scale the coupling constant sending $C \to C/r$.

The evolution of this system is shown in the right column of Fig. 5 for $r = 3$. The field moment expansion produces an accurate estimation of the field until the break time; see the rightmost column of Fig. 2. We can see that the fractional error in the field moment expansion estimation of the field is close to zero up to and past the break time. Additionally, the field moment expansion successfully predicts Q until the break time and consequently the break time itself, shown in the rightmost column of Fig. 3.

V. CONCLUSIONS

In all the test problems the FME successfully approximated the first and second order moments of the exact quantum evolution when the correction terms were subleading order, i.e., when $Q \sim 1$. Therefore, we can say that the FME provides

(1) A more accurate approximation of the expectation value of the field operator, $\langle \hat{a} \rangle$ at least until the quantum break time is as defined in Eq. (30).
(2) An accurate approximation of when the quantum break time occurs.

This is not terribly surprising because we solved the FME to second order. Intuitively, a second order approximation should remain accurate for longer than a first order approximation such as MFT. Likewise, because the benchmarks of classicality we used, the Q parameter and the PO condition, are themselves based on second order moments of the evolution, the fact that the FME can approximate the break time is not surprising.

However, it is important to note that the method makes a number of assumptions about the system. Specifically, we make an assumption about the initial conditions and the evolution of the system as follows:

(1) *Initial conditions assumption:* The initial conditions should be well approximated by the MFT. That is initially, $Q \ll 1$ and $1 - \lambda_p/n_{\rm tot} \ll 1$.
(2) *Evolution assumption:* The evolution of the field moments should be hierarchical. That is, for a term in the equations of motion of the field operators, F of order m written as a function of moments of order less than and equal to m, given F^m moments of order $\leq m$), over the evolution the terms must satisfy $F^1 > F^2 > F^3 \cdots$.

For coherent state initial conditions and the Hamiltonian in Eq. (1), these assumptions are generally satisfied. However, for initial conditions such as number eigenstates, which do not have hierarchically ordered moment terms, neither FME or MFT will accurately approximate the quantum evolution. The specific manner in which the quantum solutions approach a classical description will be explored in a later paper.

If it is known that the initial conditions of a system are well described by MFT, as in the case of coherent states, then the FME can provide a reliable check of the timescales on which the MFT approximation remains valid. This method could be applied to the evolution of ultralight scalar field dark matter created via the misalignment mechanism. Because the misalignment mechanism creates a system initially well-described by the classical theory, FME could be used to approximate the quantum break time of this system. This application will be explored in a later publication.

In this work we have focused on the results of solvers that integrate equations expanded to second order in the field moments. The equations of motion are obtained via a truncation of an infinite series of coupled differential equations. However, it may be numerically feasible to instead create a closure relation using Wick's theorem, or as is done in [14], which allows moments beyond second order to be approximated using lower order moments. Such a solver may remain accurate for longer than the current implementation.

The full code repository for the simulation and data analyses of the classical and expanded field theories performed here is publicly available at [47].

ACKNOWLEDGMENTS

A. E., A. Z., and T. A. are supported by the U.S. Department of Energy under Contract No. DE-AC02-76SF00515.

[1] M. H. Anderson, J. R. Ensher, M. R. Matthews, C. E. Wieman, and E. A. Cornell, Science **269**, 198 (1995).
[2] K. B. Davis, M.-O. Mewes, M. R. Andrews, N. J. Van Druten, D. S. Durfee, D. M. Kurn, and W. Ketterle, Phys. Rev. Lett. **75**, 3969 (1995).
[3] I. Bialynicki-Birula, Acta Phys. Austriaca Suppl. **18**, 111 (1977), https://www.osti.gov/etdeweb/biblio/5039057.
[4] W. Hu, R. Barkana, and A. Gruzinov, Phys. Rev. Lett. **85**, 1158 (2000).
[5] P. Mocz, A. Fialkov, M. Vogelsberger, F. Becerra, M. A. Amin, S. Bose, M. Boylan-Kolchin, P.-H. Chavanis, L. Hernquist, L. Lancaster, F. Marinacci, V. H. Robles, and J. Zavala, Phys. Rev. Lett. **123**, 141301 (2019).
[6] A. H. Guth, M. P. Hertzberg, and C. Prescod-Weinstein, Phys. Rev. D **92**, 103513 (2015).
[7] M. P. Hertzberg, J. Cosmol. Astropart. Phys. 11 (2016) 037.
[8] A. J. Leggett, Rev. Mod. Phys. **73**, 307 (2001).
[9] L. D. Carr, C. W. Clark, and W. P. Reinhardt, Phys. Rev. A. **62**, 063610 (2000).
[10] R. Baer, Phys. Rev. A. **62**, 063810 (2000).
[11] A. Minguzzi, S. Succi, F. Toschi, M. P. Tosi, and P. Vignolo, Phys. Rep. (2004).
[12] P. Sikivie and E. M. Todarello, Phys. Lett. B **770**, 331 (2017).
[13] O. Alon, A. Streltsov, and L. Cederbaum, Phys. Rev. A **77**, 033613 (2008).
[14] O. V. Prezhdo and Y. V. Pereverzev, J. Chem. Phys. **113**, 6557 (2000).
[15] L. Boßmann, N. Pavlović, P. Pickl, and A. Soffer, J. Stat. Phys. **178**, 1362 (2020).
[16] E. Heller, J. Chem. Phys. **64**, 63 (1976).
[17] A. Royer, Found. Phys. **22**, 727 (1992).
[18] A. Sreedharan, S. Choudhury, R. Mukherjee, A. Streltsov, and S. Wüster, Phys. Rev. A **101**, 043604 (2020).
[19] E. W. Lentz, T. R. Quinn, and L. J. Rosenberg, Mon. Not. R. Astron. Soc. **485**, 1809 (2019).
[20] E. P. Gross, Nuovo Cimento (1955–1965) **20**, 454 (1961).
[21] L. P. Pitaevskii, J. Exp. Theor. Phys. **13**, 646 (1960).
[22] A. J. Leggett, Rev. Mod. Phys. **73**, 307 (2001).
[23] B. Yurke and D. Stoler, Phys. Rev. Lett. **57**, 13 (1986).
[24] M. Lewenstein and L. You, Phys. Rev. Lett. **77**, 3489 (1996).
[25] S. Caballero-Benitez, E. Ostrovskaya, M. Gulacsi, and Y. Kivshar, arXiv:0803.4048.
[26] S. S. Chakrabarty, S. Enomoto, Y. Han, P. Sikivie, and E. M. Todarello, Phys. Rev. D **97**, 043531 (2018).
[27] S. S. Chakrabarty, Phys. Rev. D **104**, 023010 (2021).
[28] M. Kopp, V. Fragkos, and I. Pikovski, arXiv:2105.13451.
[29] G. Dvali and S. Zell, J. Cosmol. Astropart. Phys. 07 (2018) 064.
[30] G. Dvali, C. Gomez, and S. Zell, J. Cosmol. Astropart. Phys. 06 (2017) 028.
[31] E. W. Lentz, T. R. Quinn, and L. J. Rosenberg, Nucl. Phys. **B952**, 114937 (2020).
[32] L. E. Ballentine, *Quantum Mechanics. A Modern Developement* (World Scientific, Singapore, 2014).
[33] A. Georges and J. S. Yedidia, J. Phys. A **24**, 2173 (1991).
[34] A. Polkovnikov, Ann. Phys. (Amsterdam) **325**, 1790 (2010).
[35] J. Glimm, A. Jaffe, and T. Spencer, Ann. Phys. (N.Y.) **101**, 610 (1976).
[36] R. Tana and S. Kielich, Opt. Commun. **45**, 351 (1983).
[37] G. Dvali, D. Flassig, C. Gomez, A. Pritzel, and N. Wintergerst, Phys. Rev. D **88**, 124041 (2013).
[38] O. Erken, P. Sikivie, H. Tam, and Q. Yang, Phys. Rev. D **85**, 063520 (2012).
[39] A. Surez and P.-H. Chavanis, Phys. Rev. D **92**, 023510 (2015).
[40] L. Abbott and P. Sikivie, Phys. Lett. **120B**, 133 (1983).
[41] J. Preskill, M. B. Wise, and F. Wilczek, Phys. Lett. **120B**, 127 (1983).
[42] O. Penrose and L. Onsager, Phys. Rev. **104**, 576 (1956).
[43] C. Runge, Math. Ann. **46**, 167 (1895).
[44] W. Kutta, Z. Math. Phys. **46**, 435 (1901), https://www.bibsonomy.org/bibtex/24ee695c671c31151cc9816e314dfa6c2/brouder.
[45] https://github.com/andillio/QIBS.
[46] N. Aghanim *et al.*, Astron. Astrophys. **641**, A6 (2020).
[47] https://github.com/andillio/CHiMES.